Annals of Biomedical Engineering (© 2017)
DOI: 10.1007/s10439-017-1796-6

Pixel-Based DXA-Derived Structural Properties Strongly Correlate with pQCT Measures at the One-Third Distal Femur Site

ALEXANDER M. BAKER,[1] DAVID W. WAGNER,[1] B. JENNY KIRATLI,[2,3] and GARY S. BEAUPRE[1]

[1]VA Palo Alto, Musculoskeletal Research Laboratories, Palo Alto, CA, USA; [2]VA Palo Alto Health Care System, Spinal Cord Injury & Disorders Center, Palo Alto, CA, USA; and [3]Physical Medicine and Rehabilitation Division, Department of Orthopaedic Surgery, Stanford University, Stanford, CA, USA

(*Received 21 September 2016; accepted 11 January 2017*)

Associate Editor Sean S. Kohles oversaw the review of this article.

Abstract—While bone mineral density has been traditionally used to quantify fracture risk for individuals with spinal cord injuries, recent studies are including engineering measurements such as section modulus and cross sectional moment of inertia. These are almost exclusively calculated by peripheral QCT scanners which, unlike DXA scanners, are rarely found in clinical settings. Using fifty-four fresh frozen femora, we developed and validated a pixel-by-pixel method to calculate engineering properties at the distal femur using a Hologic QDR-1000 W DXA scanner and compared them against similar parameters measured using a Stratec XCT-3000 peripheral QCT scanner. We found excellent agreement between standard DXA and pixel-by-pixel measured BMD ($r^2 = 0.996$). Cross-sectional moment of inertia about the anteroposterior axis measured using DXA and pQCT correlated very strongly ($r^2 = 0.99$). Cross-sectional moment of inertia about the anteroposterior axis measured using DXA also correlated strongly with pQCT measured bone strength index ($r^2 = 0.99$). These correlations indicate that DXA scans can measure equivalent pQCT parameters, and some existing DXA scans can be reprocessed with pixel-by-pixel techniques. Ultimately, these engineering parameters may help better quantify fracture-risk in fracture-prone populations such as those with spinal cord injuries.

Keywords—BMD, DXA, DEXA, Bone QCT, Biomechanics, Osteoporosis, Fracture risk assessment, SCI, Bone Strength Index, Moment of Inertia.

INTRODUCTION

Individuals with complete spinal cord injuries (SCI) experience substantial bone loss in the lower limbs. This puts them at a high risk for fragility fractures, with the distal femur being the most common site of post-SCI facture.[8,14,41] The standard skeletal sites for osteoporosis assessment using Dual energy X-ray Absorptiometry (DXA) are the distal radius, lumbar spine and proximal femur. Unfortunately, those standard DXA scan sites have not been shown to be predictive of fractures at the distal femur or more distal sites.

The desire to assess bone density at the most common fracture sites in individuals with SCI has prompted researchers to use DXA and peripheral Quantitative Computed Tomography (pQCT) scanning protocols that specifically target regions near the knee. Garland et al. used DXA[18] to measure BMD within manually defined regions of interest located in the distal femur and the proximal tibia. Garland and colleagues subsequently proposed the use of a BMD-based "fracture threshold" to identify patients with SCI at risk of lower limb fracture.[16] To date, however, there have been no large scale studies that establish the clinical utility of a BMD fracture threshold as a reliable predictor of fracture near the knee in individuals with chronic SCI.[28]

Another commonly used imaging modality for assessing skeletal health in individuals with SCI is the use of pQCT scanners.[1,11,12,34,36] One advantage of pQCT imaging is the ability to calculate engineering parameters that reflect structural or strength-based properties, such as the moment of inertia[24] or a strength predictor such as the Bone Strength Index (BSI).[13,21] While the BSI, which is the product of the CSMI and volumetric bone density from CT, has been shown to be a very strong predictor of bone strength,[13,21] a key disadvantage of pQCT-based techniques is the relatively small number of pQCT scanners available to clinicians for routine clinical use. In 2003, Leonard[29] reported there were fewer than 100

Address correspondence to Alexander M. Baker, VA Palo Alto, Musculoskeletal Research Laboratories, Palo Alto, CA, USA. Electronic mail: alexmbaker@gmail.com

Published online: 19 January 2017

pQCT scanners in the US, compared to an estimate of more than 11,500 DXA scanners.[22] This translates to fewer than 1 pQCT scanner for every 100 DXA scanners.

The widespread availability of DXA scanners and the desire to calculate structural parameters not traditionally provided in a standard DXA analysis has fostered the development of custom software that processes individual pixel values from the projected densitometry images to calculate bone structural properties, such as the bone cross sectional area, section modulus, or moment of inertia.[6,32,33] In a pioneering 1990 study, Beck and colleagues[3] developed analysis tools for a Lunar dual photon absorptiometry scanner and a Hologic dual X-ray absorptiometry scanner. Those authors introduced a "hip strength analysis" metric that was a stronger predictor of the fracture strength of cadaver femora than was BMD ($r^2 = 0.79$ for the hip strength analysis metric vs. $r^2 = 0.63$ for BMD). Investigators collaborating with the manufacturers of DXA scanners, have subsequently developed proprietary Hip Structure Analysis (HSA) software that has been FDA-approved for use with Hologic DXA scanners,[3,26] and the proprietary Advanced Hip Assessment (AHA) software for use with GE/Lunar DXA scanners.[30,40]

Use of the HSA and AHA software has become popular with clinician scientists since they recognize that the information provided is complimentary to standard DXA measures, such as bone mineral content and bone mineral density, and it is thought that the supplemental information better reflects femoral neck strength in the form of metrics such as the cross-sectional moment of inertia, section modulus and buckling ratio.[9,19,31,35,39] HSA, in particular, has been investigated extensively at areas such as the hip[10,23] and proximal femur.[2,37] However, as the names of those software tools imply, they are specifically designed to analyze hip scans and therefore not appropriate for analyzing scans at different skeletal sites (e.g., distal femur).

The widespread availability of DXA combined with the desire to calculate structural parameters for the distal femur motivated the present study in which we had three primary objectives: (1) to develop an open-source software analysis tool that can extract and process pixel-by-pixel data from a Hologic DXA scanner; (2) to validate the new analysis software by comparing the total areal bone mineral density (aBMD) values calculated using the new software to the corresponding values output by the scanner's standard software; and (3) to calculate engineering parameters that reflect bone strength using the new analysis software and to compare those values to the values obtained from a pQCT scan.

MATERIALS AND METHODS

Fresh frozen left femora from fifty-four donors (25 male, 29 female) were scanned using a QDR-1000 W DXA scanner (Hologic, Inc., Bedford, MA, USA) and an XCT 3000 pQCT scanner (Stratec Biomedical, Birkenfeld, Germany). Femora were thawed overnight at room temperature prior to scanning. Donor characteristics and femur lengths are provided in Table 1.

For the DXA scanning, specimens were scanned in a water bath 150 mm deep to represent soft tissue.[4] Scans were performed with each femur in four rotational orientations (Fig. 1). The first scan was in the anteroposterior (AP) direction. For the second and third DXA scans, the bone was laterally and medially rotated 30° from the AP direction (AP + 30° and AP−30°, respectively) using a custom designed fixture. For the fourth scan, the bone was rotated 90°, to achieve a mediolateral (ML) orientation; the resulting projection was of the sagittal plane. All scans were performed using the spine scan mode (point spacing: 0.951 mm, line spacing: 1.003 mm). The height of the global region of interest (ROI) was 238.8 mm, with the lower end of the global ROI starting 10 mm distal to the distal-most point of the femoral condyles. Depending on the length of the femur, the global ROI covered 46% to 61% of each bone. Scan time was approximately ten minutes and all scans were performed by the same operator. Aside from segmentation procedures, the method described by Blake et al.[4] was used to extract and process data on a pixel-by-pixel basis from the Hologic data files. We refer to this approach as the "pixel-by-pixel" method. In short, the pixel-by-pixel approach uses the measured bone mass in each individual pixel to calculate its contribution to the area moment about the centroid of a bone cross section.[6,33] Taking into account all of the pixels within a given bone slice yields the density-weighted cross-sectional moment of inertia for that slice.

We used a custom-written Matlab script to extract and process the pixel-by-pixel data. For segmentation, we used an edge-detection algorithm that consisted of a combination of thresholding, spline-fitting, and region-growing to segment bone from non-bone within the global ROI.[25] This processing created pixel-based bone maps, where the BMD is known for each pixel within the segmented image.

Using pixel-by-pixel data, the total BMD was determined by averaging the BMD for all pixels within the segmented image. We compared the BMD value from the pixel-by-pixel method with the BMD value generated by the Hologic software for each AP scan. Subregional analyses were also performed over an ROI 10 mm wide, centered at a distance of 33% of the femoral length, measured from the most distal aspect of

TABLE 1. Cadaver donor characteristics.

	Male donors ($N = 25$)		Female donors ($N = 29$)	
	Mean (SD)	Range	Mean (SD)	Range
Age (years)	74.0 (9.3)	50–85	72.8 (10.6)	44–88
Height (cm)	178.3 (7.1)	167.6–190.5	162.1 (6.4)	149.9–175.3
Weight (kg)	68.4 (17.8)	41.3–118.8	64.4 (22.1)	34.0–138.8
Femur length (cm)	481.6 (17.0)	453.0–523.0	437.2 (24.8)	392.0–495.0

There were 54 specimens: 25 from male donors and 29 from female donors.

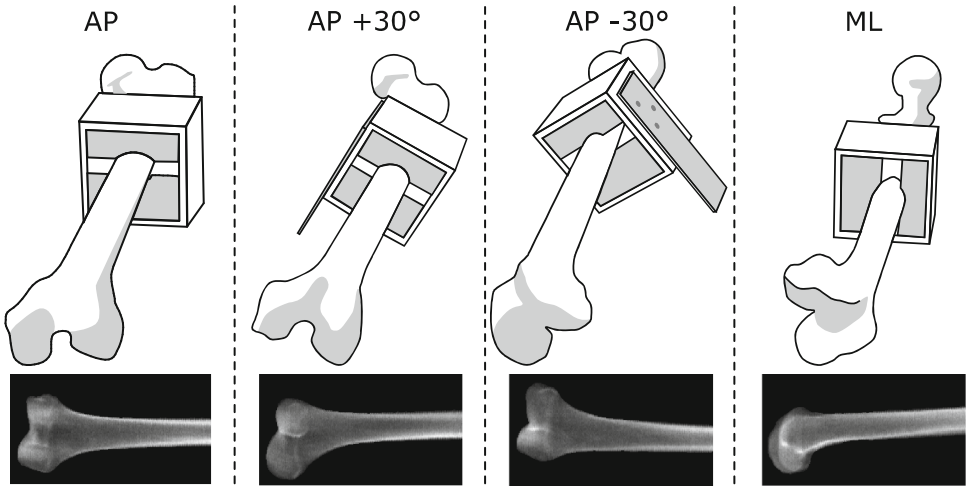

FIGURE 1. Diagram of the fixture for the four DXA scan rotations (top) and their resulting DXA scan (bottom). A rectangular side-plate was attached to the medial or lateral side of the fixture to rotate the femur +30° or −30° from AP.

the femoral condyles. The global and subregional ROIs are shown in Fig. 2. For the 10 mm wide subregional ROI, we calculated the pixel-by-pixel BMD. At the center of the subregional ROI, we calculated the density-weighted cross-sectional moment of inertia ($CSMI_{dw}$) using the method described by Martin and Burr.[33] This resulted in four values of the $CSMI_{dw}$: one about the AP axis (I_{AP}), one about an axis rotated laterally by 30 degrees (I_{AP+30}), one about an axis rotated medially by 30 degrees (I_{AP-30}) and one about the mediolateral axis (I_{ML}*). Using the method outlined by Whalen and Cleek,[6] we used the AP, AP + 30 and AP − 30 scans to calculate $CSMI_{dw}$ about the ML axis (I_{ML}). Thus the CSMI about the ML axis was both measured directly and calculated from the three CSMI values measured at the three known angles. These parameters were calculated at the center of the subregional ROI, 33% of the femoral length measured from the most distal aspect of the condyles. Because bone cross-sectional parameters do not vary rapidly along the femur diaphysis[7] we used a five-point moving average to reduce line-to-line noise. If the center of the ROI was between scan lines, a linear interpolation was used to calculate the measurements at the center of the ROI.

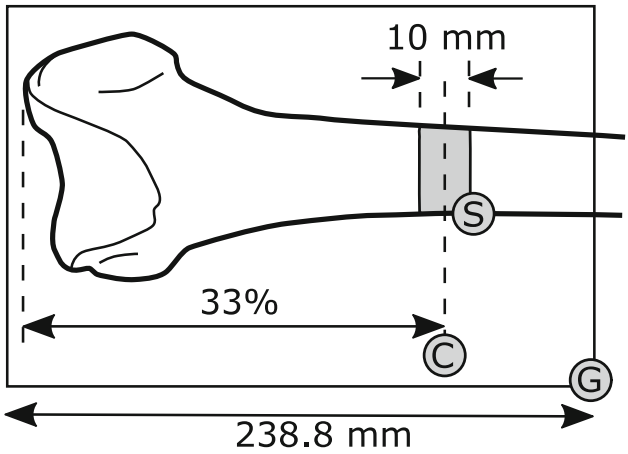

FIGURE 2. Three regions of interest and their associated measurements: (G) Global region of interest, Hologic and pixel-by-pixel BMD; (S) Subregion of interest, pixel-by-pixel BMD; (C) Centerline of subregion of interest, pixel-by-pixel and pQCT I_{AP}, and pQCT BSI.

In addition to DXA, each femur was scanned with pQCT (Stratec Medical, Pforzheim, Germany). The pixel size was 0.195 mm by 0.195 mm and the slice thickness was 2.2 mm. Each transverse slice was 4 mm apart, and a nearest-neighbor interpolation was used

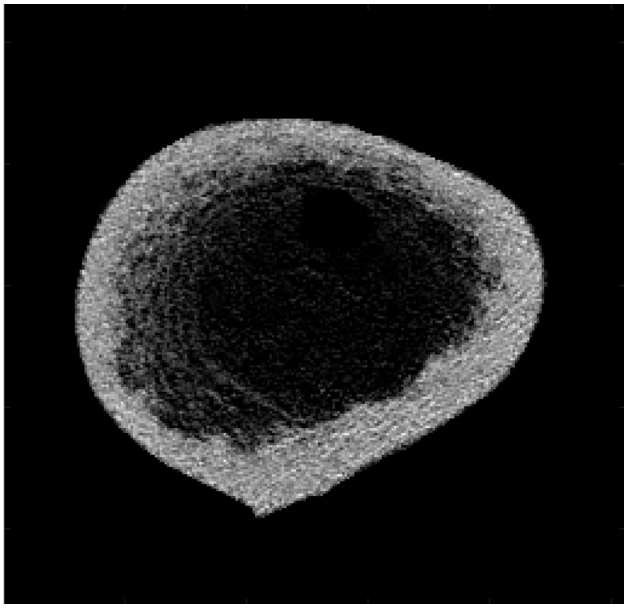

FIGURE 3. Typical pQCT cross-sectional image at the one-third region of interest. In-plane pixel size for the Stratec pQCT scans is 0.195 mm by 0.195 mm.

in between slices. The pQCT scans included the one-third ROI. Specimens were placed in a water-filled acrylic tube during scanning and all pQCT scans were performed by the same operator. A representative pQCT image at the one-third distal femur location is shown in Fig. 3. The periosteal surface was segmented manually for each scan slice. From the segmented pQCT scans, we calculated I_{AP} and the bone strength index (BSI).[13]

Statistical procedures used were least-squared linear regressions, coefficient of determination (r^2), and significance testing of regression coefficients (p). All statistics were calculated using R-3.3.2.[38]

RESULTS

The BMD calculated using the pixel-by-pixel method correlated very strongly ($r^2 = 0.996$) with the BMD reported by the Hologic software analysis (Fig. 4). Pixel-by-pixel derived I_{AP} was also strongly correlated ($r^2 = 0.99$) to I_{AP} measured using pQCT (Fig. 5).

The value of I_{ML} calculated from the pixel-by-pixel data for the AP, AP + 30, and AP − 30 scans was also very strongly correlated ($r^2 = 0.95$ $p < 0.001$) to the value for I_{ML}* measured directly from the ML scan (Fig. 6). A weak correlation was found between pixel-by-pixel BMD and BSI ($r^2 = 0.36$) (Fig. 7a), whereas a very strong correlation was found between pixel-by-pixel I_{AP} and BSI ($r^2 = 0.99$) (Fig. 7b).

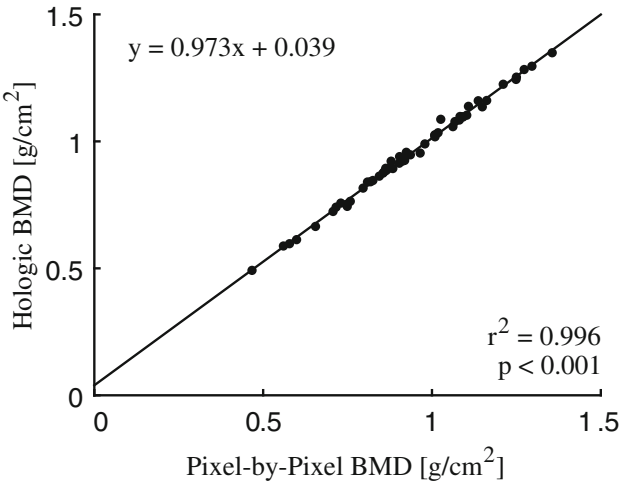

FIGURE 4. Comparison of BMD over the global region of interest measured with pQCT and DXA ($r^2 = 0.996$, $p < 0.001$).

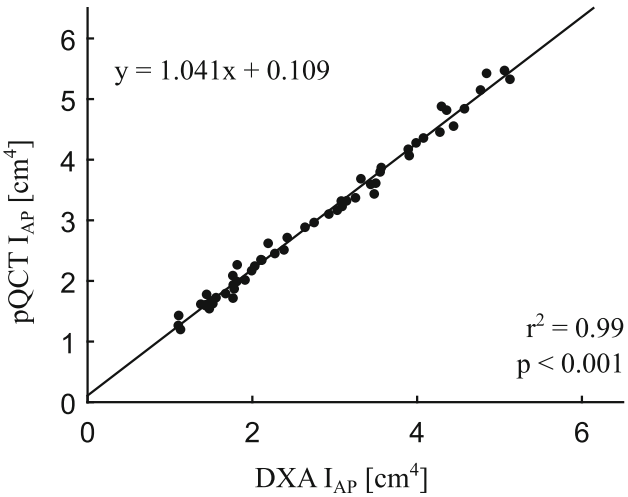

FIGURE 5. Comparison of I_{AP} at the centerline region of interest measured with pQCT and DXA ($r^2 = 0.99$, $p < 0.001$).

Regression coefficients for equivalent variables were close to, but not exactly equal to 1.0. For pixel-by-pixel BMD and Hologic BMD, the regression coefficient was significantly lower than unity (2.7%, $p = 0.004$). For pixel-by-pixel I_{AP} and pQCT I_{AP}, the regression coefficient was significantly higher than unity (4.1%, $p = 0.005$).

DISCUSSION

We developed and validated a non-proprietary pixel-by-pixel method to extract pixel-level BMD values from raw DXA scan files. When we compared the pixel-by-pixel measurements for a typical DXA parameter, BMD, with the same parameter reported by the Hologic software analysis, we found a very

strong correlation ($r^2 = 0.996$). In addition, the pixel-by-pixel method can provide engineering metrics, such as the density-weighted cross-sectional moment of inertia. Thus, pixel-by-pixel DXA can be used in place of pQCT measurements that correlate with bone strength. While pQCT provides more detail and information than DXA, the use of pQCT is limited primarily to research laboratories. DXA scanners, on the other hand, are very prevalent in clinical practice. For measurement locations pertinent to individuals with SCI, the pixel-by-pixel method can supplement standard DXA bone health measures such as Area, BMD, and BMC, with strength-based bone health measures such as I_{AP}, which may provide more information regarding fracture risk.

The values for I_{AP} from the pixel-by-pixel method were highly correlated with values of I_{AP} calculated using the pQCT scanner. This suggests that pixel-by-pixel data from a DXA scanner may be used as a substitute for pQCT to calculate I_{AP}. The value of I_{ML}, calculated from I_{AP}, I_{AP+30}, and I_{AP-30}, was strongly correlated ($r^2 = 0.95$) with I_{ML}*, which was measured directly from the DXA scan in the mediolateral direction. This corroborates the findings of Cleek and Whalen, albeit for a much larger sample size (54 specimens in the present study versus 2 specimens from a single donor).[6] Furthermore, using I_{AP} and I_{ML}, we can calculate the polar moment of inertia, I_{Polar}, which is a common measurement output from pQCT. The polar moment of inertia of the distal femur has been shown to be significantly different between individuals with SCI who sustain a fracture and those who do not.[27] While follow-up studies are still needed, I_{Polar} may help to identify individuals at risk for fracture.

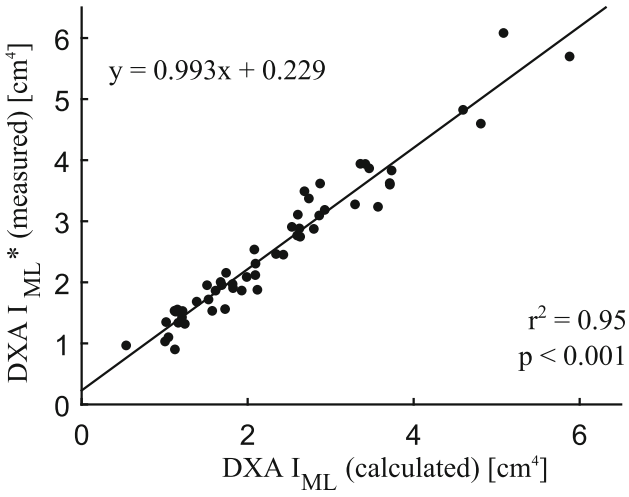

FIGURE 6. Comparison of I_{ML} calculated from three DXA scans (I_{AP}, I_{AP+30}, and I_{AP-30}) and directly measured with a DXA scan in the mediolateral direction ($r^2 = 0.95$, $p < 0.001$).

For pixel-by-pixel BMD and Hologic BMD in the global ROI, and the pixel-by-pixel I_{AP} and pQCT I_{AP} at the centerline sub-region of interest, the regression coefficients were not expected to be unity even though they are measuring the same parameters. The pixel-by-pixel method and Hologic analysis use different segmentation algorithms, and this affects their area measurements, BMC measurements, and subsequently their BMD measurements. The difference in regression coefficients between the DXA I_{AP} and the pQCT I_{AP} were also expected because DXA and pQCT are different scanning modalities, and each modality has inherent biases. The strength parameter BSI is almost exclusively calculated using pQCT. This is because the calculation of BSI requires knowledge of the volumetric bone density, which DXA, by virtue of its two-dimensional nature, is unable to provide without making additional assumptions about the geometry of the scanned bone. Even so, pixel-by-pixel I_{AP} is very highly correlated with the strength parameter BSI

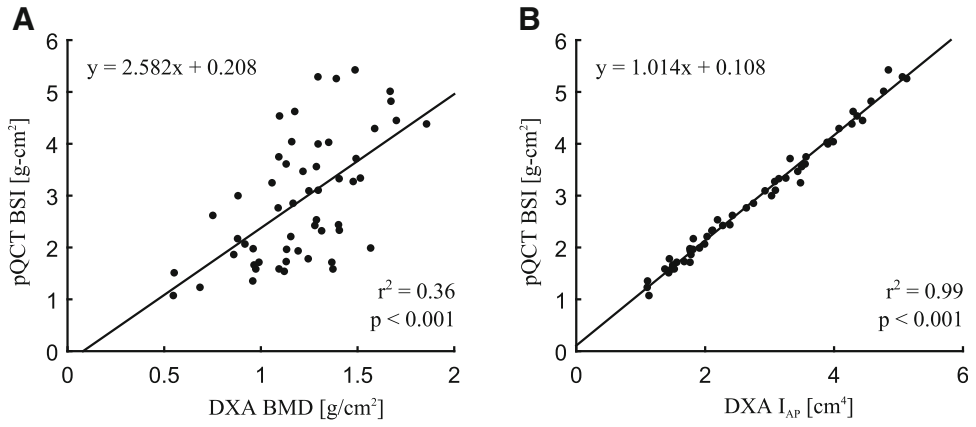

FIGURE 7. (a) Comparison of Bone Strength Index measured with pQCT and BMD measured with DXA ($r^2 = 0.36$, $p < 0.001$); (b) Comparison of Bone Strength Index measured with pQCT and I_{AP} measured with DXA ($r^2 = 0.99$, $p < 0.001$). The significant difference in correlation coefficients suggests that I_{AP} offers additional information over BMD.

($r^2 = 0.99$). On the other hand, BMD is only weakly correlated with BSI ($r^2 = 0.36$). The most significant implication of these results is that pixel-by-pixel derived DXA parameters may be used in place of pQCT measurements to assess bone strength in the distal femur. While pQCT images have more detail and information than DXA, their use is limited primarily to research laboratories and are seldom found in clinical use. DXA scanners, on the other hand, are very prevalent in clinical practice. For measurement locations pertinent to individuals with SCI, clinical densitometry can more readily transition from standard DXA bone health measures such as Area, BMD, and BMC, into strength-based bone health measures such as $I_{AP,}$ or BSI which may provide more information regarding fracture risk.

Ultimately, and most importantly, by using the pixel-by-pixel method, it is possible to reanalyze and reinterpret the results from existing DXA-based studies on fracture-relevant locations, such as the distal femur or tibia.[15,17] While we cannot calculate rotationally independent parameters such as I_{Polar} from existing scans because the femur is typically scanned in the AP direction only, the single-scan parameter I_{AP} is strongly correlated with pQCT strength measurements, such as the BSI. Data previously obtained from longitudinal studies, representing measurements made over many years, as well as cross-sectional studies, which may involve large cohorts, could be reprocessed using our method to yield results comparable to pQCT strength measurements that have been shown to correlate highly with bone strength.[13] We would, however, advise caution in reanalyzing sub-regions extracted from whole body scans. Whole body scans are typically performed using larger pixels (larger point spacing and line spacing) than regional (forearm, spine, hip) scans, and one would expect diminished accuracy in bone edge detection as well as data smoothing with larger pixels from whole body scans. We would recommend a re-validation of the pixel-by-pixel approach to determine the accuracy of the derived engineering metrics before reanalyzing sub-regions from pre-existing whole body scans. However, the pixel-by-pixel method applies only to the Hologic QDR-1000 W, and other scanners will require different software. Looking forward, future studies should create similar pixel-by-pixel methods for other DXA scanners such as the Hologic and GE/Lunar fan beam scanners.. We encourage manufacturers to release tools to derive these pixel-by-pixel maps for research use. Additionally, as some modern scanners include an X-ray detector – emitter system that can rotate, intended for performing a mediolateral scan of the spine, we feel that this is a great opportunity for scanners to automatically derive rotation-independent parameters, such as the polar moment of inertia.

We note that all of our scans were performed *ex vivo* with excised femora. *In vivo* measurements generally have lower precision due to inconsistency of soft tissue attenuation, which is caused by an indeterminate lean-to-fat soft tissue ratio.[4,5] While *in vivo* scans have precision better than 3% for BMD,[20] this high precision may not hold for the structural parameters we calculate. Future studies will need to address these precision issues with cadaver specimens containing intact soft tissue or with clinical subjects before introducing strength measurements into clinical diagnostics.

In summary, we developed a non-proprietary method to calculate pixel-by-pixel BMD maps from raw DXA scan files, and from those pixel-by-pixel BMD maps, we were able to calculate a parameter, I_{AP}, which was highly correlated with equivalent pQCT parameters in the distal femur, I_{AP} and BSI. Our results suggest that DXA-derived strength measures can be used in place of pQCT-derived strength measures, which, due to the prevalence of clinical DXA scanners, may be more convenient for clinical usage. Additionally, these DXA-pQCT correlations make it possible to reinterpret existing DXA-based studies involving individuals with SCI using a bone-strength approach to bone health assessment. Future work should extend the pixel-by-pixel method to other models of DXA scanners, and use this pixel-by-pixel method to reprocess existing DXA scan data.

The code used in this study for the pixel-by-pixel analysis, referred to as VA-DXAMOI, is available from http://simtk.org/home/va-dxamoi.

ACKNOWLEDGMENTS

Funding for this work was provided by the Department of Veterans Affairs, Rehabilitation R&D Service (Proj. F0920-P). We thank Christine Dairaghi for performing the DXA and pQCT scans and for manual segmentation of the periosteal surface in the pQCT images. We are also indebted to Dr. Robert Whalen, Dr. Tammy Cleek, and Dr. Glen Blake for their invaluable assistance in understanding the architecture and processing of the Hologic scan files.

REFERENCES

[1]Ashe, M. C., J. J. Eng, A. V. Krassioukov, D. E. Warburton, C. Hung, and A. Tawashy. Response to functional

electrical stimulation cycling in women with spinal cord injuries using dual-energy X-ray absorptiometry and peripheral quantitative computed tomography: a case series. *J. Spinal Cord Med.* 33:68–72, 2010.

[2]Beck, T. J., A. C. Looker, C. B. Ruff, H. Sievanen, and H. W. Wahner. Structural trends in the aging femoral neck and proximal shaft: analysis of the third national health and nutrition examination survey dual-energy X-ray absorptiometry data. *J. Bone Miner. Res.* 15:2297–2304, 2000.

[3]Beck, T. J., C. B. Ruff, K. E. Warden, W. W. Scott, and G. U. Rao. Predicting femoral neck strength from bone mineral data. A structural approach. *Invest. Radiol.* 25:6–18, 1990.

[4]Blake, G. M., D. B. McKeeney, S. C. Chhaya, P. J. Ryan, and I. Fogelman. Dual energy x-ray absorptiometry: the effects of beam hardening on bone density measurements. *Med. Phys.* 19:459–465, 1992.

[5]Bolotin, H. H. Inaccuracies inherent in dual-energy X-ray absorptiometry in vivo bone mineral densitometry may flaw osteopenic/osteoporotic interpretations and mislead assessment of antiresorptive therapy effectiveness. *Bone* 28:548–555, 2001.

[6]Cleek, T. M., and R. T. Whalen. Cross-sectional structural parameters from densitometry. *J. Biomech.* 35:511–516, 2002.

[7]Cleek, T. M., and R. T. Whalen. Effect of activity and age on long bones using a new densitometric technique. *Med. Sci. Sports Exerc.* 37:1806–1813, 2005.

[8]Comarr, A. E., R. H. Hutchinson, and E. Bors. Extremity fractures of patients with spinal cord injuries. *Am. J. Surg.* 103:732–739, 1962.

[9]Culafić, D., D. Djonic, V. Culafic-Vojinovic, S. Ignjatovic, I. Soldatovic, J. Vasic, T. J. Beck, and M. Djuric. Evidence of degraded BMD and geometry at the proximal femora in male patients with alcoholic liver cirrhosis. *Osteoporos. Int.* 26:253–259, 2015.

[10]Danielson, M. E., T. J. Beck, A. S. Karlamangla, G. A. Greendale, E. J. Atkinson, Y. Lian, A. S. Khaled, T. M. Keaveny, D. Kopperdahl, K. Ruppert, S. Greenspan, M. Vuga, and J. A. Cauley. A comparison of DXA and CT based methods for estimating the strength of the femoral neck in post-menopausal women. *Osteoporos. Int.* 24:1379–1388, 2013.

[11]Dudley-Javoroski, S., and R. K. Shields. Longitudinal changes in femur bone mineral density after spinal cord injury: effects of slice placement and peel method. *Osteoporos. Int.* 21:985–995, 2009.

[12]Eser, P., A. Frotzler, Y. Zehnder, and J. Denoth. Fracture threshold in the femur and tibia of people with spinal cord injury as determined by peripheral quantitative computed tomography. *Arch. Phys. Med. Rehabil.* 86:498–504, 2005.

[13]Ferretti, J. L., R. F. Capozza, and J. R. Zanchetta. Mechanical validation of a tomographic (pQCT) index for noninvasive estimation of rat femur bending strength. *Bone* 18:97–102, 1996.

[14]Freehafer, A. A., C. M. Hazel, and C. L. Becker. Lower extremity fractures in patients with spinal cord injury. *Spinal Cord* 19:367–372, 1981.

[15]Garland, D., and R. Adkins. Bone loss at the knee in spinal cord injury. *Top. Spinal Cord Inj. Rehabil.* 6:37–46, 2001.

[16]Garland, D., R. Adkins, and C. Stewart. Fracture threshold and risk for osteoporosis and pathologic fractures in individuals with spinal cord injury. *Top. Spinal Cord Inj. Rehabil.* 11:61–69, 2005.

[17]Garland, D. E., R. H. Adkins, C. A. Stewart, R. Ashford, and D. Vigil. Regional osteoporosis in women who have a complete spinal cord injury. *J. Bone Jt. Surg.* 83:1195–1200, 2001.

[18]Garland, D., Z. Maric, R. Adkins, and C. Stewart. Bone mineral density about the knee in spinal cord injured patients with pathologic fractures. *Contemp. Orthop.* 26:375, 1993.

[19]Haskelberg, H., N. Pocock, J. Amin, P. R. Ebeling, S. Emery, and A. Carr. Hip structural parameters over 96 weeks in HIV-infected adults switching treatment to tenofovir-emtricitabine or abacavir-lamivudine. *PLOS ONE* 9:e94858, 2014.

[20]Ilich, J. Z., L. C. Hsieh, M. A. Tzagournis, J. K. Wright, M. Saracoglu, H. S. Barden, and V. Matkovic. A comparison of single photon and dual X-ray absorptiometry of the forearm in children and adults. *Bone* 15:187–191, 1994.

[21]Jämsä, T., P. Jalovaara, Z. Peng, H. K. Väänänen, and J. Tuukkanen. Comparison of three-point bending test and peripheral quantitative computed tomography analysis in the evaluation of the strength of mouse femur and tibia. *Bone* 23:155–161, 1998.

[22]Kanis, J. A., and O. Johnell. Requirements for DXA for the management of osteoporosis in Europe. *Osteoporos. Int.* 16:229–238, 2004.

[23]Kaptoge, S., N. Dalzell, N. Loveridge, T. J. Beck, K.-T. Khaw, and J. Reeve. Effects of gender, anthropometric variables, and aging on the evolution of hip strength in men and women aged over 65. *Bone* 32:561–570, 2003.

[24]Kontulainen, S. A., J. D. Johnston, D. Liu, C. Leung, T. R. Oxland, and H. A. McKay. Strength indices from pQCT imaging predict up to 85% of variance in bone failure properties at tibial epiphysis and diaphysis. *J. Musculoskelet. Neuronal Interact.* 8:401–409, 2008.

[25]Kourtis, L. C., D. R. Carter, H. Kesari, and G. S. Beaupre. A new software tool (VA-BATTS) to calculate bending, axial, torsional and transverse shear stresses within bone cross sections having inhomogeneous material properties. *Comput. Methods Biomech. Biomed. Engin.* 11:463–476, 2008.

[26]LaCroix, A. Z., T. J. Beck, J. A. Cauley, C. E. Lewis, T. Bassford, R. Jackson, G. Wu, and Z. Chen. Hip structural geometry and incidence of hip fracture in postmenopausal women: what does it add to conventional bone mineral density? *Osteoporos. Int.* 21:919–929, 2010.

[27]Lala, D., B. C. Craven, L. Thabane, A. Papaioannou, J. D. Adachi, M. R. Popovic, and L. M. Giangregorio. Exploring the determinants of fracture risk among individuals with spinal cord injury. *Osteoporos. Int.* 25:177–185, 2013.

[28]Lala, D., B. C. Craven, L. Thabane, A. Papaioannou, J. D. Adachi, M. R. Popovic, and L. M. Giangregorio. Exploring the determinants of fracture risk among individuals with spinal cord injury. *Osteoporos. Int.* 25:177–185, 2014.

[29]Leonard, M. B. Assessment of bone health in children and adolescents with cancer: promises and pitfalls of current techniques. *Med. Pediatr. Oncol.* 41:198–207, 2003.

[30]Leslie, W. Short-term precision and cross-calibration for GE advanced hip assessment. *J. Clin. Densitom.* 18:429, 2015.

[31]Litwic, A. E., M. Clynes, H. J. Denison, K. A. Jameson, M. H. Edwards, A. A. Sayer, P. Taylor, C. Cooper, and E. M. Dennison. Non-invasive assessment of lower limb geometry and strength using hip structural analysis and peripheral quantitative computed tomography: a population-based comparison. *Calcif. Tissue Int.* 98:158–164, 2016.

[32]Lou Bonnick, S. H. S. A. Beyond BMD with DXA. *Bone* 41:S9–S12, 2007.
[33]Martin, R. B., and D. B. Burr. Non-invasive measurement of long bone cross-sectional moment of inertia by photon absorptiometry. *J. Biomech.* 17:195–201, 1984.
[34]McCarthy, I. D., Z. Bloomer, A. Gall, R. Keen, and M. Ferguson-Pell. Changes in the structural and material properties of the tibia in patients with spinal cord injury. *Spinal Cord* 50:333–337, 2012.
[35]Mochizuki, T., K. Yano, K. Ikari, K. Kawakami, R. Hiroshima, N. Koenuma, M. Ishibashi, and T. Shirahata. Hip structure analysis by DXA of teriparatide treatment: A 24-month follow-up clinical study. *J. Orthop.* 13:414–418, 2016.
[36]Ooi, H. L., J. Briody, M. McQuade, and C. F. Munns. Zoledronic acid improves bone mineral density in pediatric spinal cord injury. *J. Bone Miner. Res.* 27:1536–1540, 2012.
[37]Petit, M. A., H. A. Mckay, K. J. Mackelvie, A. Heinonen, K. M. Khan, and T. J. Beck. A randomized school-based jumping intervention confers site and maturity-specific benefits on bone structural properties in girls: a hip structural analysis study. *J. Bone Miner. Res.* 17:363–372, 2002.
[38]R Core Team. R: a language and environment for statistical computing. Vienna, Austria: R Foundation for Statistical Computing, 2016. https://www.R-project.org/.
[39]Sone, T., M. Ito, M. Fukunaga, T. Tomomitsu, T. Sugimoto, M. Shiraki, T. Yoshimura, and T. Nakamura. The effects of once-weekly teriparatide on hip geometry assessed by hip structural analysis in postmenopausal osteoporotic women with high fracture risk. *Bone* 64:75–81, 2014.
[40]Takakuwa, M., K. Otsuka, M. Konishi, and K. Itabashi. Evaluation of the effect of 4 months of risedronate therapy on femoral strength using femoral strength analysis tools. *J. Int. Med. Res.* 37:1972–1981, 2009.
[41]Vestergaard, P., K. Krogh, L. Rejnmark, and L. Mosekilde. Fracture rates and risk factors for fractures in patients with spinal cord injury. *Spinal Cord* 36:790–796, 1998.